Experimental investigation and modelling of a buoyant attached plane jet in a room

Guangyu Cao, J. Kurnitski, M. Ruponen, O. Seppänen

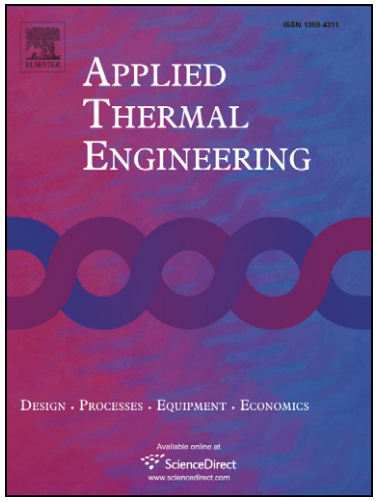

Experimental investigation and modelling of a buoyant attached plane jet in a room

Guangyu Cao, J. Kurnitski, M. Ruponen, O. Seppänen

PII: S1359-4311(09)00053-2
DOI: 10.1016/j.applthermaleng.2009.01.016
Reference: ATE 2735

To appear in: *Applied Thermal Engineering*

Received Date: 9 July 2008
Revised Date: 23 January 2009
Accepted Date: 24 January 2009

Please cite this article as: G. Cao, J. Kurnitski, M. Ruponen, O. Seppänen, Experimental investigation and modelling of a buoyant attached plane jet in a room, *Applied Thermal Engineering* (2009), doi: 10.1016/j.applthermaleng.2009.01.016

Experimental investigation and modelling of a buoyant attached plane jet in a room

Guangyu Cao [a,*], J. Kurnitski [a], M. Ruponen [b], O. Seppänen [a]

[a] *Department of Mechanical Engineering, Helsinki University of Technology, 02150 ESPOO, Finland*

[b] *Halton Oy, Haltonintie 1-3, 47400 Kausala, Finland*

Abstract

Buoyant attached jets are widely used in various types of supply air devices especially in office buildings. This study focuses on a two-dimensional cooled attached jet characteristic, including mean flow field structure, specification of the jet regions and maximum velocity decay. A new superimposing model is derived to predict the maximum velocity decay and validated by measurement results. The measurement results demonstrate that the intermediate region of a buoyant jet does exist when an inner layer extends downstream of the jet slot. In addition, by assuming that the buoyant force is the main extra force on the jet flow in the acceleration process, the superimposing model predicted the maximum velocity decay with precise accuracy in a Reynolds number range of 667-4000, based on slot heights of 20 and 30 mm and slot velocities of 0.50, 1.00 and 2.00 m/s. At a distance of 1000 mm from the slot, the velocity profile displays a self similarity character like an isothermal turbulent jet. In the final region, where the buoyancy flux completely dominates the jet, the jet behaved like a plume with an unstable flow field.

Keywords: Buoyant; Attached plane jet; Modelling; Velocity decay; Jet region

1. Introduction

The turbulent attached plane jet, also called the plane wall jet, has been applied in ventilated and air conditioned space for many years. In isothermal conditions, the jet behavior is well understood regarding both the structure and mechanisms [1-4]. However, non-isothermal conditions pose a challenging problem in the prediction of the buoyant attached jet behavior. One of the attached jet applications in rooms is the active chilled beam which enables a plane jet discharging on the ceiling so that the high-velocity region is restricted to the ceiling, thus possibly freeing the occupied zone from draught [5-6]. Under normal design conditions, the jet stays attached to the ceiling until the opposite wall is reached, when it is then deflected downwards into the wall-floor zone. Hence, the maximum jet velocity should be predicted accurately to control the local draught rate in a room by the attached plane jet.

* Corresponding author. Tel.: +358 9 4513796; Fax: +358 9 4513611.
Email address: gcao@cc.hut.fi (G.Y. CAO)

Fig. 1 shows the division of the buoyant jet into three regions: the non-buoyant region, the intermediate region and the buoyant region. The earlier study showed that the non-buoyancy region refers to the same region as a jet 'starting length' [7]. Basically, the jets in a quiescent ambient can be classified according to the relative importance of the initial momentum flux and the initial specific buoyancy flux [8]. In addition, it has been found that relative influence of inertia and buoyancy forces resolves the stratified flow characteristics in a room [9].

At present, different computational fluid dynamics (CFD) simulation models were developed and implemented in turbulent jet studies from small scale to fully scale simulation [10-11]. However, the validation of the CFD models could be case dependent in the engineering applications [12-17]. Moreover, the experimental studies were always carried out to validate the jet models or the CFD simulation results in the jet flow investigations. The experimental method is still considered as a reliable way to directly study the jet behaviors and characteristics in many cases.

Nomenclature

Latin symbols

a	acceleration (m^2/s)
b	coefficient of the non buoyant zone model
Ar	Archimedes number
F_b	buoyancy force (N)
g	gravitational acceleration (9.81 m^2/s)
h	air jet slot height (m)
K	coefficient which will depend on the slot Reynolds number if less than 10^4
K^e	coefficient of buoyant jet due to temperature difference
L_{non}	distance of the non-buoyant region
P_c	total cooling power (W)
P_h	heat load power of thermal dummies (W/m^2)
q_s	supply air flow rate (L/s)
Q	air volume flow (L/s)
Re	Reynolds number
T_0	initial jet temperature (°C)
T_a	jet ambient air temperature (°C)
T_j	jet temperature (°C)
T_{ref}	buoyancy reference temperature
T_s	supply air temperature (°C)
T_w	wall surface temperature (°C)
T_∞	room temperature (°C)
$u_m(x)$	local maximum air velocity at a distance x from the jet slot (m/s)
U_0	slot average air velocity (m/s)
$u_m^{lb}(x)$	local buoyant jet maximum velocity (m /s)
x	jet horizontal traveling distance (m)
x_0	distance to virtual origin (m)
x_p	jet potential core distance (m)
y	vertical distance from initial point (m)
$y_{1/2}$	the value of y at which the velocity u is half its center-line value

Greek symbols

ρ	density of fluid (kg/m^3)
υ	kinematic viscosity ($m^2 \cdot s^{-1}$)
δ	boundary layer thickness
δQ	supply air uncertainty (%)
δT	measurement room temperature uncertainty (%)
δu_x	measured velocity uncertainty (%)
δu	anemometer uncertainty (%)
δx	measurement location uncertainly (%)
θ	temperature
η	equal to $y/y_{1/2}$

Subscripts

1,2,3	coefficient number
a	ambient air
c	cooling
j	jet
0	jet slot
p	potential core
ref	buoyancy reference
s	jet slot
t	turbulent
w	wall surface

In previous studies, the correlations of the buoyant jet penetration distance were derived from the experimental results [18] and the heat transfer between the wall and the jet was clarified experimentally [19]. Meanwhile, different empirical and theoretical models were established and validated to predict the jet velocity distribution [20-24]. Recent investigations into the buoyant attached jet were conducted by the application of the chilled beam [25-26]. In fact, the jet equation derived from the free jet case is used to calculate the jet maximum velocity in the practical designing [21]. It is known that the coefficient of square root of two could be used in the attached jet model [27]. The original jet model takes the expression as:

$$\frac{u_m(x)}{U_0} = \left[\frac{Kh}{x}\right]^{0.5} \pm \sqrt{\frac{KAr_0}{0.2}\left(2.83 \cdot \sqrt{\frac{x}{Kh}} - 1\right)} \qquad (1)$$

where $u_m(x)$ is the, K=5 was supposed in [23]. The Eq. (1) was called modified Regenscheit model. The Ar_0 is the slot Archimedes number defined as:

$$Ar_0 = \frac{gh(T_s - T_\infty)}{T_h U_0^{\ 2}} \qquad (2)$$

The purpose of this study was to create a practical, one-jet-equation model which can be used in both preliminary stage of the attached plane jet devices development and in room air distribution design, i.e. in ventilation or air conditioning design. This study has the potential to contribute to the development of the chilled beam, one of the low velocity attached jet applications (range from 0.5-2.0 m/s), which could provide good energy performance, excellent thermal comfort and silent operation [28-30]. Here, the two dimensional condition was assumed for the attached plane jet as a starting point. It should be also noted that the studied case was as much 2D as it can be in engineering applications.

The main aim of this study was to obtain detailed data and knowledge of the mean flow

field of a buoyant attached plane jet in a room. The specific objectives were:

1) to describe the flow field structure influenced by the buoyancy force over the wall surface by means of measurement;
2) to set up an effective model to predict the maximum velocity decay;
3) to validate the maximum jet velocity model in a range of Reynolds numbers based on slot velocities of 0.50, 1.00 and 2.00 m/s;
4) to verify the self similarity characteristic of the buoyancy jet in three different jet regions.

2. Derivation of the buoyant superimposing jet velocity model

2.1 Boundary conditions

Here, the non-slip condition is applied on the wall surface which bounds the attached plane air jet. The following boundary conditions are:

$$u = v = 0 \quad at \quad y = 0$$

and

$$u = v = 0 \quad at \quad x = \infty, y = \infty$$

For the cooling jet over the well insulated wall surface, the heat flux between the wall and the jet could be neglected. Thus:

$$q_w = 0 \quad at \quad y = 0$$

$$T_w = T_{jet} \quad at \quad y = 0$$

The above thermal boundary condition was presented also in [31].

2.2 Buoyancy Superimposing Model

Earlier study showed a superimposing method to predict the maximum velocity of the attached plane jet in the near wall zone [27]. Here, a new buoyant superimposing model is set up to predict the maximum jet velocity decay which consists of the isothermal part and the buoyant part. The isothermal part can be expressed by the jet similarity equation:

$$u_m(x) = U_0 D_1 (x + x_0)^p \tag{3}$$

where p represents the unknown value of the similarity exponents; and -0.48 and -0.5 were reported as suitable value for jet application [32-34].

However, experimental studies show that the jet similarity does exist but may be expressed in a alternate way by using different similarity exponents. The relationship between the local maximum velocity and the downstream position could be expressed as [35]:

$$u_m(x) = D_2 (x + x_0)^b \tag{4}$$

where b is the similarity exponent. The averaged b in Eq. (4) is proven to be -0.555 by experimental results. In other studies, it was even found that the incomplete similarity exponent, -0.6, exists between the inner and outer zones [36-37].

Here, the similarity exponent, 0.55, in the isothermal part of superimposing model is used in Eq. (3). The relationship between the jet virtual origin and the jet slot Reynolds number is known [32]:

$$\frac{x_0}{h} = D_3 + D_4 \,\mathrm{Re} \tag{5}$$

The jet slot Reynolds number is defined as:

$$\mathrm{Re} = \frac{U_0 h}{\nu} \tag{6}$$

The parameters, D3 and D4, were determined by two points test data. Here 0.54 and 0.0021 are used in Eq. (5). After substitution of *D3* and *D4*, Eq. (6) becomes:

$$\frac{x_0}{h} = 0.54 + 0.0021\mathrm{Re} \tag{7}$$

A simplified analysis was carried out for a small bulk of air jet to derive the second part of the model. The buoyancy force acting vertically on a certain volume of air flow, Q, with temperature T and density ρ which are different from those of the surrounding fluid T_0 and ρ_0 , is

$$F_b = Q \; g(\rho_0 - \rho) \tag{8}$$

The air density could be inversely proportional to the air temperature as: $\rho \propto 1/T$. Then Eq. (8) becomes

$$F_b = Q \; g\rho\left(\frac{T}{T_0} - 1\right) \tag{9}$$

The buoyant force produces a vertical acceleration a expressed as:

$$a = \frac{F_b}{Q\rho} \tag{10}$$

Substituting for F_b yields

$$a = \frac{g\Delta T}{T_0} \tag{11}$$

where $\Delta T = T - T_0$

If the vertical distance between this given volume and a reference point is x, then the volume airflow will move vertically at a velocity, u

introduced to represent the additional buoyant velocity relative to the reference point as:

$$\left(u^{'}\right)^2 = 2xa \tag{12}$$

Substituting for a from Eq. (10), obtain:

$$\left(u^{'}\right)^2 = \frac{2gx\Delta T}{T_0} \tag{13}$$

Then

$$u^{'} = \left(\frac{2gx\Delta T}{T_0}\right)^{1/2} \tag{14}$$

Eq. (14) presents the velocity due to the buoyancy force acting vertically on a unit volume of a different temperature from the surroundings. Here, a temperature decay coefficient, K^e, is introduced to calculate the buoyancy acceleration velocity at a distance of x downstream to the jet slot. Then Eq. (15) takes the expression with K^e as:

$$u^{'} = \left(K^e \frac{gx\Delta T}{T_0}\right)^{1/2} \tag{15}$$

Combining the isothermal velocity and the buoyancy velocity, the superimposing model becomes:

$$u_m^{lb}(x) = u_m(x) + u^{'} = U_0 D_1 (x + x_0)^p + \left(K^e \frac{gx\Delta T}{T_0}\right)^{1/2} \tag{16}$$

The parameters D_1 and K^e are determined by one point test data. Preliminary test show that D_1 takes 0.51 and 0.70 for the cases with 20 mm and 30 mm slot height and K^e uses 0.53 for cases by both slot heights.

The superimposing model consisting of Eq. (3) to Eq. (16) could be applied by using the following assumptions: 1) the air entrained by the jet has a room air temperature; 2) the only force opposing the jet is the wall shear stress and the free shear stress; 3) the turbulent jet momentum in the mixing process is approximately preserved; 4) the attached-plane-jet with a low Reynolds number has a similar similarity exponent to the high Reynolds number jet.

3. Experimental facilities and instrument

3.1 The test chamber

Fig. 2 displays the layout of the test chamber and measurement point distribution. The test chamber consists of a well insulated wall mounted with a jet supply device and nine adjustable dummies specified in [38].

Fig. 3 shows the cross section of the air supply device and the measured jet flow field. The supplied air is ducted by a variable-speed frequency-controlled centrifugal fan.

3.2 Measurement conditions

In the measurement, various jet velocities, ranging from 0.50 to 2.00 m/s, can be obtained by regulation of the outflow restriction from 30 to 120 L/s. The turbulence intensity at the slot exit center is approximately 0.95%. Table 1 displays the six experimental conditions.

Table 1 Experimental condition in the six measured cases

Slot height	*Slot V(m/s)*	q_s [L/s]	ΔT [°C]	T_{Supply} [°C]	T_{Room} [°C]	P_c [W]	P_h [W]	*Re*	Ar_0
20 mm	0.50	20	-3	20.0±0.2°C	23.0±0.2°C	-72±7	72	667	0.007954
	1.00	40	-3	20.5±0.2°C	23.5 ±0.2°C	-144±14	144	1333	0.001985
	2.00	80	-3	20.0±0.2°C	23.0±0.2°C	-288±29	288	2667	0.000497
30 mm	0.50	30	-3	19.0±0.2°C	22.0 ±0.2°C	-108±11	108	1000	0.003661
	1.00	60	-3	18.6±0.2°C	21.6±0.2°C	-216±22	216	2000	0.000916
	2.00	120	-3	18.9±0.2°C	21.9 ±0.2°C	-432±43	432	4000	0.000229

3.3 Measurement instrument and accuracy

In this study, the mean jet velocities have been measured using seven omni-directional spherical anemometers. The probe of the omni-directional spherical anemometer has a 2 mm diameter. The digital HT400 recording system collects signals of anemometer and thermometer with frequency 5 Hz. The anemometers have upper frequency 0.5 Hz by which it means that it can properly measure velocity changes slower than 0.5 Hz [39-40]. All these anemometers were calibrated using TSI's Model 8392 Certifier Air Velocity Calibrator. Table 2 shows the summary of the instruments accuracy.

Table 2 Accuracy of the measurement instruments

	Accuracy			
Velocity (m/s)	Anemometer	Temperature sensor	Supplied air	Traversing device
1.25-7.5	2.0% of reading ±0.025 (m/s)	±0.1(°C)	±3.6 (L/s) (3.0% of supply air)	± 1 mm
0.15-1.25	2.0% of reading ±0.01 (m/s)	±0.1°C	±1.8 L/s(3.0% of supply air)	± 1 mm

In addition, the measurement error sources may include the directional sensitivity of the anemometer, the dynamic response of the anemometer, and temperature gradients in the flow [41].

4 Results

4.1 Mean velocity field

During the measurement, the velocity is recorded every second and the average velocity is obtained over each three-minute period.

Fig. 4 shows the whole downstream jet structure. At the 0.50 m/s slot velocity, the jet structure is slightly turbulent. When increase the slot velocity from 0.50 to 2.00 m/s, the whole jet flow field looks like a laminar flow.

Fig. 5 displays that the whole jet flow field resembles a more laminar-like structure than in the case of the 20 mm slot height. By using 10% of the slot velocity as the outermost layer velocity, the whole jet thickness is then confined by the wall surface and the line with 0.05, 0.1 and 0.2 m/s.

4.2 Predicted maximum jet velocity

In this section, the calculation results by the modified Regenscheit model (Eq. 1) and the superimposing model (Eq. 16) are compared with the measured results in six cooling cases.

Fig. 6 displays the measured and calculated centerline velocity decay. These results indicate that the calculated results by the superimposing model fit closely to the measured data with only marginal errors. Most of the results by the modified Regenscheit model scatter outside the margins of the measurement result.

4.3 Velocity profiles

To clarify the difference between different buoyant jet regions, the measured velocity profiles are collected and compared with the theoretical turbulent velocity profile by the equation derived by Schwarz and Cosart [35]:

$$\frac{u(x)}{u_m(x)} = \exp\left[-0.937(\eta - 0.14)^2\right] \quad (17)$$

Fig. 7 depicts measured velocity profiles and theoretical profiles. By 0.50 m/s slot velocity with 20 mm slot height, the measured velocity profile fits the theoretical profile closer at the distance of 2000 mm than the distance of 1000 mm and 3000 mm from the jet slot.

5 Discussions

5.1 The buoyant jet regions

By the definition of the three regions in the buoyant jet structure, Fig. 4 shows that there have no obvious distinguishing points that could separate the three regions of the buoyant jet. At different slot jet velocities, the inner layer attached to the wall surface could be observed below the jet center line. The measurement results show that the intermediate region of the buoyant jet does exist when the inner layer extends downstream of the jet slot. The furthest distance that the inner layer extended is approximately 500, 1500 and 2500 mm in Fig. 4, corresponding to 0.50, 1.00 and 2.00 m/s slot average velocities, respectively. The existence of intermediate region of the buoyant jet defined by So and Aksoy [8] indicates this situation as the initial momentum flux and the buoyancy flux are of comparable importance.

The last region (buoyant region) could be considered as the region beyond the intermediate region at a certain distance downstream of the slot. In Fig. 4, the buoyant region will cover the region further than 500, 1500 and 2500 mm corresponding to 0.50, 1.00 and 2.00 m/s slot velocities, respectively. During the transition from intermediate region to buoyant region, Fig. 4 shows an acceleration trend of the downward jet flow caused by buoyancy force along the wall surface. In the buoyant region, the jet structure displays a somewhat turbulent character at a distance of 2000, 2500 and 3000 mm downstream of the slot.

5.2 Self similarity of the buoyant jet

Comparisons with the measured data demonstrate that the superimposing model is validated for slot velocities from 0.50 m/s to 2.00 m/s. However, at the beginning of the jet flow and after 2000 mm downstream to the slot, the error between the calculated results and measurement data appears. On the basis of the classification of buoyant jet regions, the different characteristics of the three regions in the buoyant jet might contribute to the error. Moreover, the size and the details of the jet outlet could also contribute to the discrepancy between the predicted results and the measured results. Malmström [42] states that the outlet can influence the velocities and temperatures in the resulting jet through three different mechanisms: momentum gains or losses, jet spread and the form of temperature profile.

As defined in [6-7], if the relative influence of momentum and buoyancy are used as the critical criteria to classify the flow regions, the non-buoyancy region refers to the situation in which momentum dominates the jet behavior. Then the jet behaves like a plume rather than a jet with a certain structure. The similarity characteristic differs from isothermal jet behavior [36]. Abdulhadi [31] and Quintana [34] already confirmed that the buoyant jet has the characteristics of self-similarity within a distance of 12 to 50 slot heights downstream of the jet slot.

Fig. 7 indicates that the distance of non-buoyant region might be proportional to the slot Reynolds number and inversely proportional to the initial Archimedes number. The relationship between the distance of the non-buoyant region, the slot Reynolds number and initial Archimedes number could be formulated as:

$$L_{non} = b_1 \mathrm{Re} + \frac{b_2}{Ar} + b_3 \qquad (18)$$

Within the non-buoyant region, the maximum velocity may be calculated by the isothermal jet equation. Beyond this region, the superimposing model may be applied to predict the maximum velocity decay. To test this hypothesis, more measurements are needed for the determination of each coefficient in Eq. (18).

6 Conclusions

In a vertical non-isothermal turbulent buoyant jet, the measurement results illustrate that different flow regions can be identified at some distance downstream of the jet exit. The distance of each region could be dependent on the initial conditions, including the slot Reynolds number and the initial Archimedes number. At different slot jet velocities, the inner layer attached to the wall surface are observed below the jet center line. A higher initial Archimedes number and lower slot Reynolds number could contribute to the thicker jet and more turbulent outer layer. The observation of the extended inner layer confirms that the intermediate region of the buoyant jet does exist when the initial momentum and the buoyancy flux are of comparable importance. In the buoyant region, when the buoyancy flux completely dominates the jet, the jet behaves like a plume with an unstable flow field.

The superimposing model is derived and validated by the measurement results. The superimposing model could predict accurately the maximum velocity decay beyond the non-buoyant region in the range of 667-4000 Reynolds number, which is based on a slot size of 20 and 30 mm and slot velocity of 0.50, 1.00 and 2.00 m/s. The modified Regenscheit model failed to predict the non-isothermal jet maximum velocity decay with a lower Reynolds number less than 4000.

The measurement results demonstrate that the velocity profile displays a self similarity character like an isothermal turbulent jet at the point 1000 mm from the slot. The profile with a 2 m/s slot velocity fits the theoretical profile very well. To specify the starting point of the buoyant region, more detailed measurement results may be needed.

The data obtained in the work could be used to validate the responding CFD simulation for further product development. The superimposing model established here potentially could be used as a practical one-equation method to predict the jet maximum decay in the preliminary stage of product development, and in room air distribution design especially by attached plane jet application, i.e. chilled beam. In addition, at a given or expected room air velocity, the data and the model specified in this study could be applied to improve the accuracy of the calculation by CFD software.

Acknowledgment

The authors wish to express their appreciation for the measurement support provided by Halton Oy and for the financial support kindly provided by Halton Oy, the Finnish association of HVAC societies and K.V. Lindholm Foundation of Finland.

References

[1] N. Rajaratnam, B.S. Pani, Three-dimensional turbulent wall jet, in: Proceedings of the A.S.C.E., J. Hydraul. Div. 100 (1974) 69-83.
[2] N.Rajaratnam, Turbulent Jets. Elsevier, Amsterdam, 1976.
[3] B.E. Launder, W. Rodi, The turbulent wall jet - measurements and modeling, Annual review of fluid mechanics 15 (1983) 429-459.
[4] H.B. Awbi, Ventilation of Buildings. London, Chapman & Hall, 1991.
[5] J. Fredriksson, M. Sandberg, B. Moshfegh, Experimental investigation of the velocity field and airflow pattern generated by cooling ceiling beams, Build. Environ. 36 (2001) 891-899.
[6] H. Yu, C.M. Liao, H.M. Liang, K.C. Chiang, Scale model study of airflow performance in a ceiling slot-ventilated enclosure: Non-isothermal condition, Build. Environ. 42 (2007) 1142-1150.
[7] J.C. Chen, W. Rodi, Turbulent buoyant jets — A review of experimental data, HMT, Pergamon, London, 1980.
[8] R.M.C. So, H. Aksoy, On vertical turbulent buoyant jets, Int. J. Heat Mass Transfer 36(13) (1993) 3187-3200.
[9] A.S. Awad, R.K. Calay, O.O. Badran, A.E. Holdo, An experimental study of stratified flow in enclosures, Applied Thermal Engineering 28 (2008) 2150–2158
[10] L.K. Voigt, Comparison of turbulence models for numerical calculation of airflow in an annex 20 Room, Report ET-AFM 2000-01, Technical University of Denmark, ISBN 87-7475-225-1.
[11] E. Baydar, Y. Ozmen, An experimental and numerical investigation on a confined impinging air jet at high Reynolds numbers, Applied Thermal Engineering 25 (2005) 409–421.
[12] Q. Chen, Comparison of different k-ε models for indoor air computations, Numerical heat transfer 28 (1995) 728-734.
[13] J. Srebric, Q. Chen, L.R. Glicksman, Validation of a zero-equation turbulence model for complex indoor airflow simulation. ASHRAE Transactions RP-927 (1999) 414-427.
[14] T. Karimipanah, Turbulent jets in confined spaces, PhD thesis, Centre for Built Environment, Royal Institute of Technology, Gävle, Sweden, 1996.
[15] S.L. Sinha, R.C. Arora, S. Roy, Numerical simulation of two dimensional room air flow with and without buoyancy, Energy and Build. 32 (2000) 121–129.
[16] P.G. Tucker, Y. Liu, Turbulence modeling for flows around convex features giving rapid eddy distortion, International Journal of Heat and Fluid Flow 28 (2007) 1073–1091.
[17] K.Z. Yu, G.L. Ding, T.J. Chen, Simulation of air curtains for vertical display cases with a two-fluid model, Applied Thermal Engineering 27 (2007) 2583–2591.
[18] K. Sato, H. Osuka, I. Inoue, Maximum penetration distance of a vertical buoyant jet, International Chemical Engineering 21(3) (1981) 435-443.
[19] J.W. Yang, R.D. Patel, Effect of buoyancy on forced convection in a two-dimensional wall jet along a vertical wall, Journal of Heat Transfer 95 (1) (1973) 121-123.
[20] M. Grimitlyn, Zurluftverteilung in raumen. Luft und Kältetechnik 5 (1970) 246-256.
[21] B. Regenscheit, Strahlgesetze und Raumströmung. Klima-Kälte-Technik 6, 1975.
[22] W. Moog, Dimensionierung von Luftführungssystemen. Fortschritt-Berichte Der Zeitschriften 6 (49) 1978.
[23] K. Klobut, J. Palonen, Ilmasuihkut Kirjallisuuskatsaus, Technology report, Helsinki, 1992.
[24] S. Rama, G. Reddy, Combined natural and forced convection in a laminar wall jet along a vertical plate with uniform surface heat flux, Appl. Sci. Res. 31(6) (1976) 455-463.
[25] G.Y. Cao, J. Kurnitski, P. Mustakallio, O. Seppänen, Performance of chilled beam air distribution close to the wall, in: Proceedings of the 10th International Conference on Air Distribution in Rooms, Helsinki, Finland, 2007.
[26] G.Y. Cao, J. Kurnitski, P. Mustakallio, O. Seppänen, Chilled Beam's air distribution measurements and plane wall jet modeling, in: Proceedings of the 5th International Symposium on Heating, Ventilating and Air Conditioning, Beijing, China 2007, pp. 288-295.
[27] G.Y. Cao, J. Kurnitski, P. Mustakallio, O. Seppänen, Active Chilled Beam Wall Jet Prediction by the Free Convection Model, International Journal of Ventilation 7(2) (2008) 169-178.
[28] F. Alamdari, D.J.G. Butler, P.F. Grigg, M.R Shaw, Chilled Ceilings and Displacement Ventilation, Renewable Energy 15 (1998) 300-305.
[29] B. Costelloe, D. Finn, Indirect evaporative cooling potential in air–water systems in temperate climates, Energy and Build. 35(6) (2003) 573-591.
[30] S.B. Riffat, X. Zhao, P.S. Doherty, Review of research into and application of chilled ceilings and displacement ventilation systems in Europe, Int. J. Energy Res. 28 (2004) 257–286.
[31] R. Abdulhadi, C.O. Pedersen, The behavior of a downward-directed heated wall jet. ASHRAE Transactions 2 (1971) 222-229.
[32] R.A. Bajura, A.A. Szewczyk, Experimental investigation of a laminar two-dimensional attached plane jet, Phys Fluids 13(7) (1970) 1653-166.
[33] M.B. Glauert, The wall jet, J Fluid Mech 1 (1956) 625-643.
[34] D.L. Quintana, M. Amitay, A. Ortega, Heat Transfer in the Forced Laminar wall jet, Journal of Heat Transfer 119 (1997) 451-458.
[35] W. H.Schwarz, W.P. Cosart, The two-dimensional turbulent wall jet, J. Fluid Mech. 10 (1961) 481-495.
[36] G.I. Barenblatt, A.J. Chorin, V.M. Prostokishin, The turbulent wall jet: A triple-layered structure and incomplete similarity, in: Proceedings of the Natl Acad Sci U S A 102(25) (2005) 8850–8853.
[37] R.I. Karlsson, J. Eriksson, J. Persson, In Laser Techniques and Applications in Fluid Mechanics: Selected Papers from the 6th Int. Symposium on Applications of Laser Techniques to Fluid Mechanics, 1992.
[38] DIN4715-1, Chilled surfaces for rooms- Part 1: Measuring of the performance with free flow – Test rules, November 1995.
[39] A.K. Melikov, Z. Popiołek, F. E. Jorgensen, New method for testing dynamic characteristics of low velocity thermal anemometers. ASHRAE Transactions 104(1b) (1998) 1490-1506.
[40] T. Stannov, A.K. Melikov, Z. Popiołek, F. E. Jorgensen, Test method for describing directional sensitivity of anemometers for low-velocity measurements indoors. ASHRAE Transactions 104(1b) (1998) 1481-1489.
[41] A.K. Melikov, Z. Popiolek, M.C.G. Silva, I. Care, T. Sefker, Accuracy limitations for low-velocity measurements and draft assessment in rooms, HVAC & R Research 13(6) (2007) 971-986.
[42] T.G. Malmström, Archimedes number and jet similarity, in: Proceedings of the 5th International conference on air distribution in rooms, Yokohama, Japan, 1996, pp. 415-422.

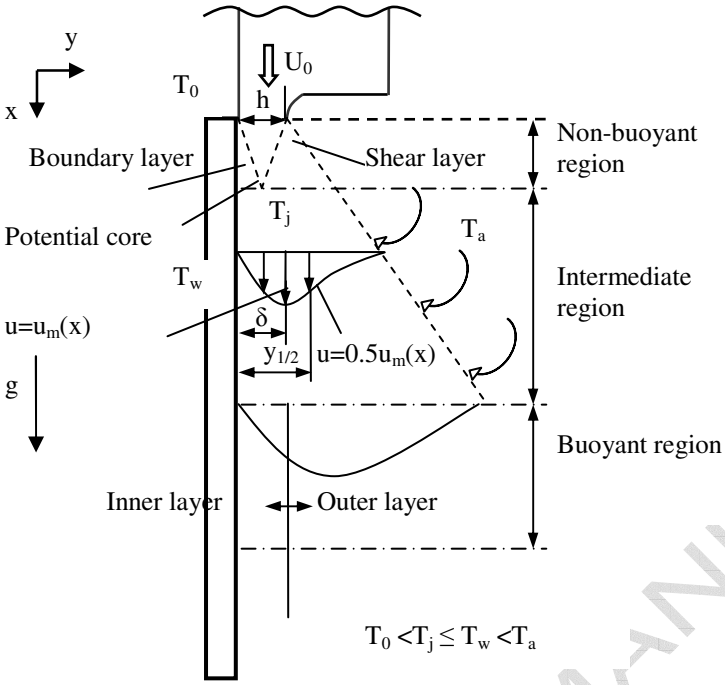

T_0 initial jet temperature,
T_j jet temperature,
T_w wall surface temperature and,
T_a ambient air temperature

Fig. 1. Schematic of the attached buoyancy jet

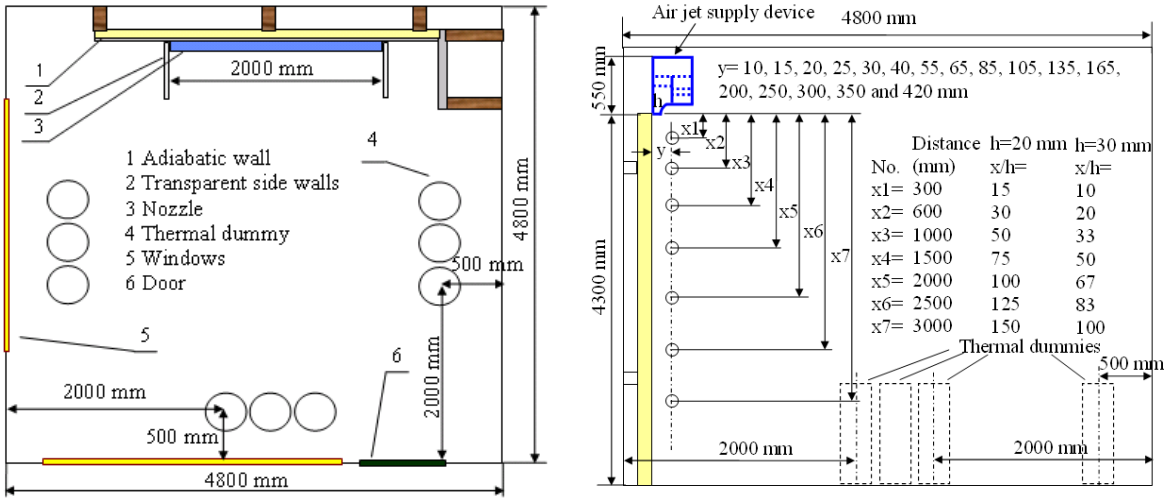

a) layout of the chamber with locations of air supply device and thermal dummies

b) measurement point distribution

Fig. 2. Test chamber layout and measurement point distribution

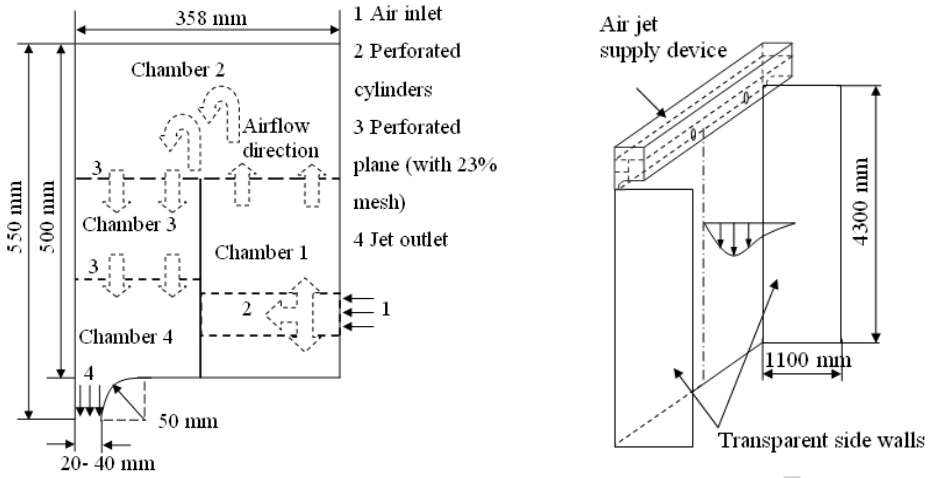

a) cross-sectional view of the vertical air supply device

b) the attached jet flowfield for measurement

Fig. 3. Schematic view of experimental setup

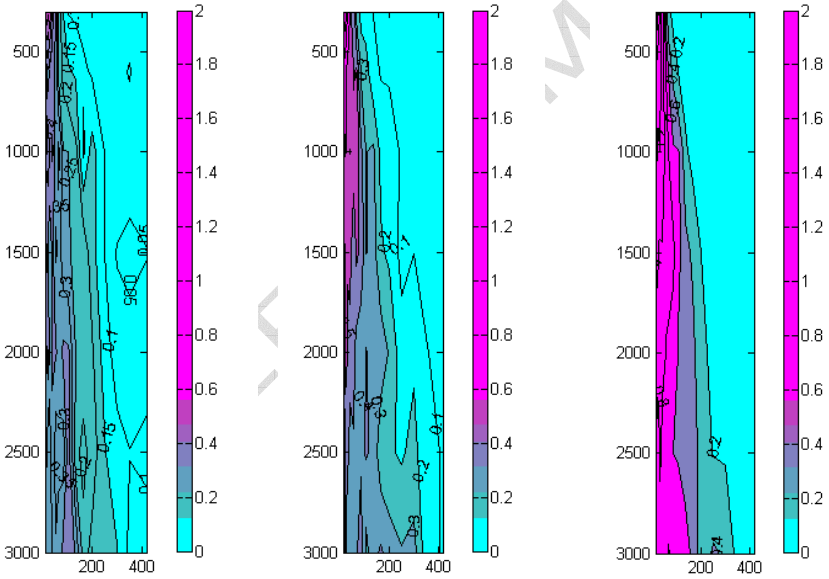

0.50 m/s at slot 1.00 m/s at slot 2.00 m/s at slot

Fig. 4. Air velocity distributions for -3 degree cooling jet with 20 mm slot height

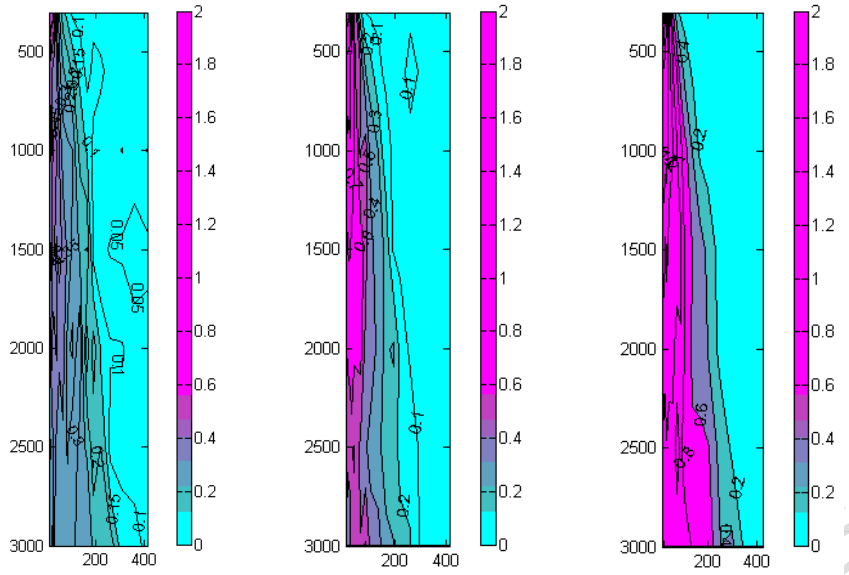

0.50 m/s at slot 1.00 m/s at slot 2.00 m/s at slot

Fig. 5. Air velocity distributions for -3 degree cooling jet with 30 mm slot height

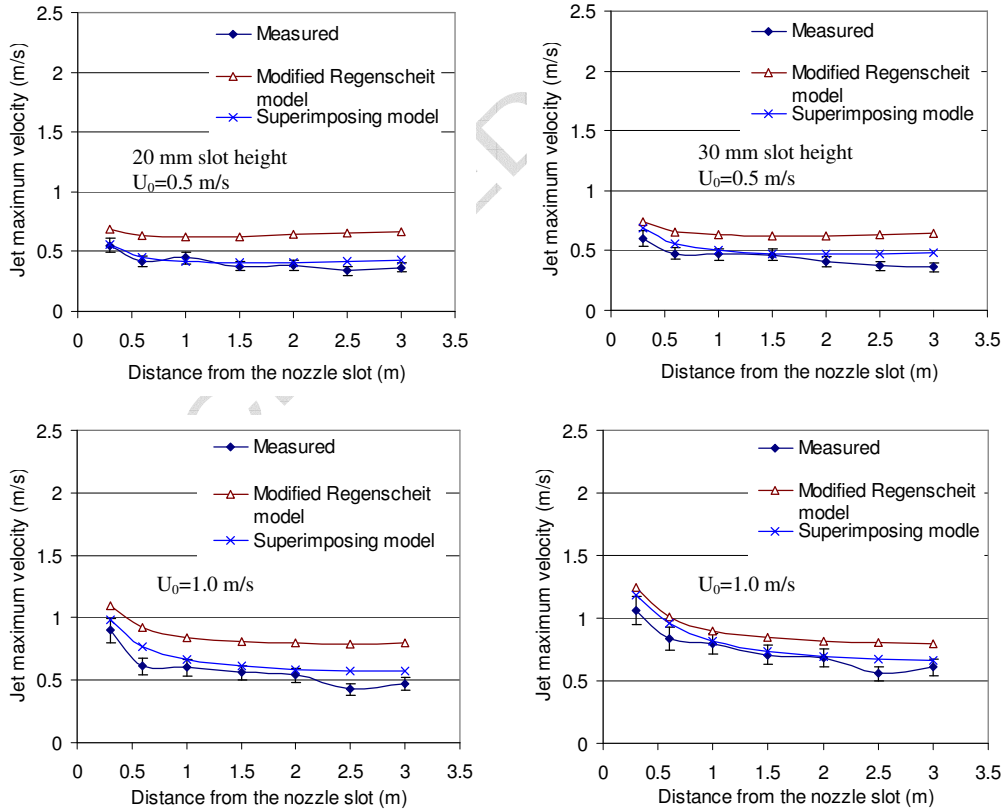

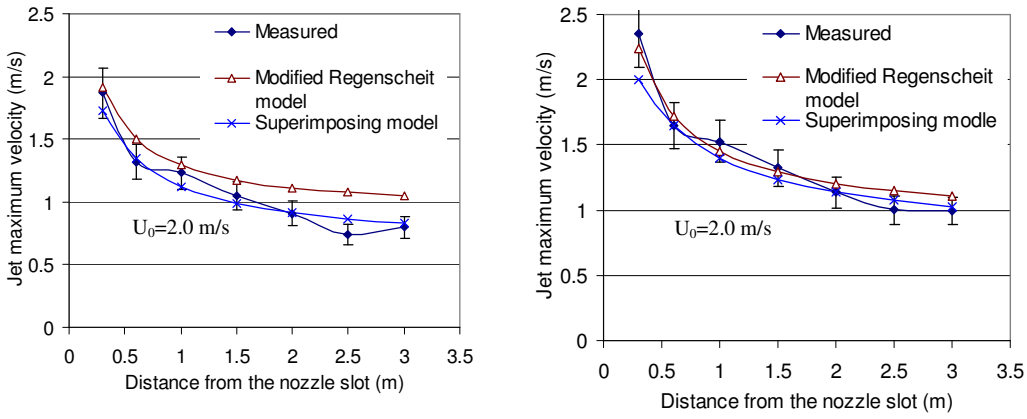

Fig. 6. Measured and calculated centerline velocity decay

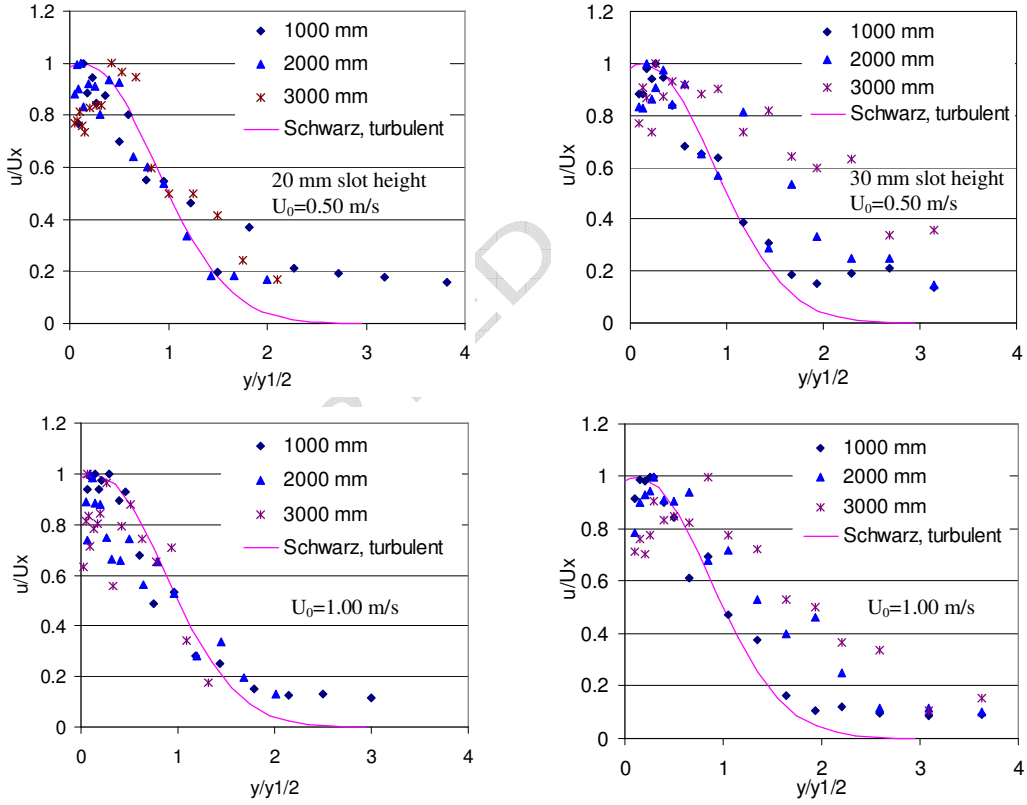

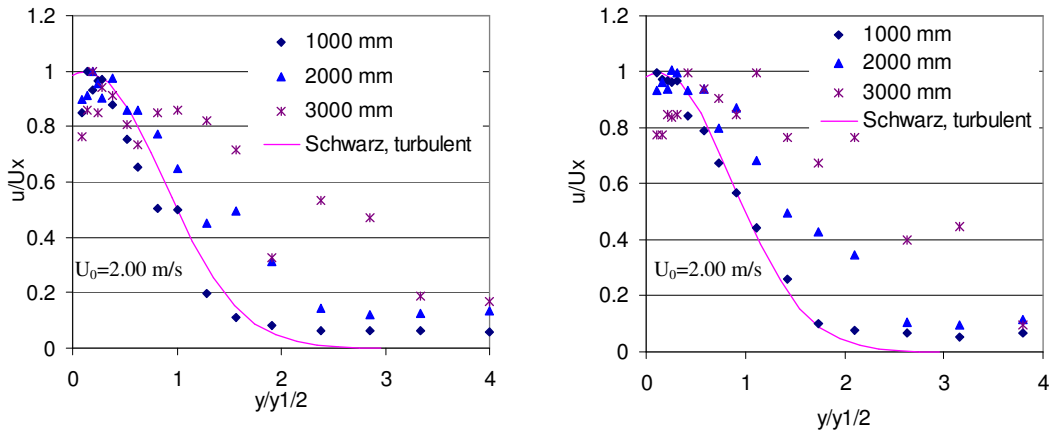

Fig.7. Measured velocity profiles and theoretical profiles